92-52

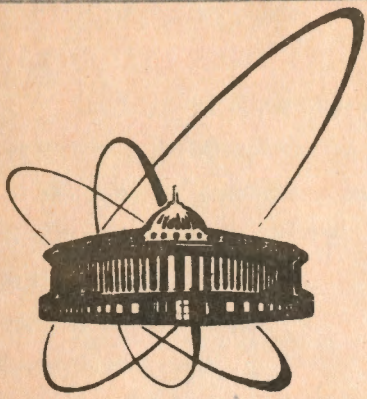

объединенный
институт
ядерных
исследований
дубна

E13-92-52

G.A.Cheremukhina, S.P.Chernenko, A.B.Ivanov,
V.I.Mikerov[2], T.Netusil[1], A.I.Ostrovnoi,
A.Wisinger[1], Yu.V.Zanevsky

A TWO-DIMENSIONAL DETECTOR WITH DELAY LINE READOUT FOR SLOW NEUTRON FIELDS MEASUREMENTS

Submitted to "Nuclear Instruments and Methods"

[1]Permanent address: National Research Institute for Materials, Opletalova 25, 113 12 Prague, Czechoslovakia
[2]Lebedev Physical Institute of Academy of Science of Russia, Leninsky Prospect 53, 117924 Moscow, RF

1992

Черемухина Г.А. и др.
E13-92-52

Двумерный детектор со съемом данных
с помощью линий задержки
для измерения полей медленных нейтронов

Описаны двумерный детектор медленных нейтронов и электроника съема координатной информации и накопления данных на основе ПК/АТ. Двумерный детектор, с чувствительной площадью 260 X 140 мм, собран на основе многопроволочной пропорциональной камеры высокого давления со съемом с помощью линий задержки и заполняется смесью 3 атм. ^{3}He и пропана. Собственное пространственное разрешение детектора составляет 1,4 мм (ПШПВ) и 1,9 мм (ПШПВ) для 2,2 атм. и 1,5 атм. пропана соответственно. Эффективность регистрации нейтронов выше 80% (λ = = 6Å), однородность по площади лучше 2,6%. Быстродействие координатного детектора нейтронов $\geqslant$ 200 кГц полезных событий.

Работа выполнена в Лаборатории высоких энергий ОИЯИ.

Препринт Объединенного института ядерных исследований. Дубна 1992

Cheremukhina G.A. et al.
E13-92-52

A Two-Dimensional Detector with Delay Line Readout
for Slow Neutron Fields Measurements

This article presents the description of a two-dimensional detector of slow neutrons together with its readout and data acquisition electronics based on a PC/AT. The detector with a sensitive area of 260 X140 mm^2 is based on a high pressure multiwire proportional chamber with delay line readout and gas filling of 3.0 atm. ^{3}He + propane. The intrinsic spatial resolution of the detector is either $\cong$ 1.4 mm (FWHM) or 1.9 mm (FWHM) for 2.2 atm. and 1.5 atm. of propane, respectively. The detection efficiency is more than 80% (λ = 6Å) at the uniformity less than 2.5%. Count rate capability of the neutron detector is not less than 2.0 X10^5 among the selected events.

The investigation has been performed at the Laboratory of High Energies, JINR.

Preprint of the Joint Institute for Nuclear Research. Dubna 1992

1. INTRODUCTION

Studies of structures with $1 \div 10^4$ Å in size have attracted nowadays considerable interest in various fields of science: in physics of condensed matter, biology, chemistry, geology. There are various objects of interest in these studies: thin layers, multilayer systems, biological membranes and molecular aggregates, liquid crystals, synthetic and natural polymers, superconductors [1 ÷ 2]. Among conventional methods of structural studies, the neutron methods are irreplaceable [3] due to penetrating properties of neutrons through matter. First of all, it refers to small-angle neutron scattering (SANS), as well as small-angle neutron reflectometry (SANR), which are more and more intensively used, and, besides, to conventional neutron diffraction. Measurements done with the mentioned methods or by industrial applications (neutron radiography and tomography) lead to measurements of a count in many points of the resulting neutron field. Conventional scanning by means of the neutron counter with a narrow slit, cannot fully satisfy requirements of these methods. It takes a lot of time and summs the radiation background. A modern experimental instrument based on the SANS and SANR is characterized by a data acqusition system based on a position-sensitive detector (PSD) of neutrons [3].

PSD for neutron scattering experiments are of various size, shapes and posses different detection parameters: spatial (angle) resolution , count rate, detection efficiency or non-sensitivity to gamma background. All kinds of radiation detectors (gaseous, scintillation, semiconductor, solid

state) are used to perform sensitive detection of neutron position. The principles of work and parameters of many neutron PSD are presented in the review [4]. The requirements to a neutron PSD depend on the facility used for the designed experiment. It should be emphasized that at the present time gaseous detectors with ^{3}He filling are used more often in the experiments. The application of neutron PSD improves parameters of the experimental set-up, reduces the measuring time significantly and increases reliability of results.

A two-dimensional detector of slow neutrons together with readout electronics and data acquisition system has been developed at JINR (Dubna), the pressure vessel was fabricated in FIAN (Moscow). It is used for digital registration of neutron fields in SANS, SANR and diffraction experiments at the multipurpose diffraction facility DNM-1, which has been constructed in FIAN, Moscow. The detection system is based on two-dimensional detector with high resolution because of narrow scattering angles at the above-mentioned experiments ($2\Theta < 10^{o}$). The multipurpose diffraction facility DNM-1 includes a small-angle diffractometer and a standard one, besides, a two-crystal monochromator, several focusing slit collimators, cryogenic and termic chambers, etc. The neutron wavelength changes from 1 to 20 $\mathring{A}$ and the neutron beam intensity doesn't excess 10^5 neutrons/s. at the horizontal neutron channel of the IRT MIFI reactor (Moscow) where the DNM-1 facility is situated.

Due to the limited size of the experimental area, the spatial resolution less than 3 mm (FWHM) is needed. In general, at neutron scattering experiments the long term

detection stability is required and the detection sensitivity for gamma-radiation should be as low as possible, but the detection efficiency for slow neutrons must be maximum. As far as the neutron flux in the experimental beam at a steady state reactor almost reaches 10^5 neutrons/s, high count rate (over 10^5) of the selected events/s is required. These requirements have been taken into account when the detector and readout electronics were designed.

2. NEUTRON PSD

A two-dimensional detector described below is based on a standard multiwire proportional chamber (MWPC) with a delay line (DL) coordinate readout [5]. The readout method used in the work fulfils all the main requirements and it was chosen due to a priveous good experience [6,7].

The detector together with electronics is designed for digital registration of a spatial distribution of neutron fields counting each neutron separately and determining its coordinates simultaneuosly. A schematic view of the detector with electronics is shown in fig.1.

The neutron PSD consists of :

- a two-dimensional MWPC, placed in a sealed aluminium vessel and working at high pressure in a gas mixture based on ^{3}He,
- readout electronics and data acquisition system designed for coordinate readout of events from MWPC and data acquisition using a histogramming memory connected with a PC/AT.
- PC/AT compatible computer with the software to

control the data acquisition system, perform preliminary data prosessing and displaying the neutron field

2.1 Construction of the detector

The detector, standard MWPC, is placed in the sealed aluminium vessel with inner sizes 500 x 360 x 22 mm^3. The vessel consits of two parts: a base plate and a cover with a recess of 270 x 140 mm^2 outside to provide a 6 mm thick input window for neutrons. The neutron scattering in the input window should be less than 5% (at $\lambda = 6$ Å). The base plate together with the cover is sealed by the indium wire. A temporary sealing in the preliminary experiments has been accomplished by a simple vacuum rubber "O" ring, the gas leakage was less than 0.05 atm/month at a pressure of 4.5 atm. Since the input window serves as a drift space electrode, it has to be flat within 0.25 mm. The larger deformation would result in noticeable nonuniformities of the detection efficiency. The window deflects less than 0.2 mm at the gas pressure of 6 atm.

A view of the detector without the cover is shown in fig.2. All electrode frames of fibreglass with stretched wires are assembled together and pushed to the base plate by means of a metalic frame. Preamplifiers and high voltage [H.V.] networks are placed on the opposite side of the base plate and connected with the MWPC via glass feedthroughs. Valves and a pressure gauge are connected via extension tubes to the upper side of the base plate. It allows to handle and control gas when the detector is installed inside borated polyethylene shielding box.

The MWPC has a sensitive area of 320 x 190 mm^2, but due to the construction of the input window the sensitive area for neutrons is somewhat smaller, up to 260 x 140 mm^2. The electrode geometry of the detector is illustrated in fig.3. It consists of the flat MWPC, supplemented by two drift gaps (input window- $cathode_x$ and $cathode_y$-drift electrode-2). The sensitive volume for neutron conversion has the total thickness of 21 mm. Spacing between adjacent electrode planes is 4.0 mm with exception of the gap between drift electrode-1 and drift electrode- 2, which is 5 mm. Drift electrode-2 is made by coating the bottom of vessel base plate by a 0.8 mm thick STEF insulator covered with copper foil. The anode electrode is streched with gold-plated tungsten wires of 20-μm diameter with 2 mm spacing. Anode wires are all connected together to obtain the total energy signal, which is used for the background discrimination and gating of coordinate readout electronics. All the other electrodes are of Be-Cu wires of 50-μm with 1.0 mm spacing. Cathode wires are soldered on the printed circuit boards and interconnected in groups of four. Each wire group is soldered to one of two delay lines to obtain a specific delay of the interconnection τ = 1.0 ns per mm of the corresponding coordinate. Signals from each end of every delay line are led to its low-noise preamplifier with the input impedance of about 300Ω, which is close to the delay line impedance.

The detector is operated by means of two high voltage power supplies. A high positive potential up to 6.5 kV can be put on the anode. Cathodes together with delay lines are held

at a positive potential, too, corresponding to 30 % of the anode potential which is obtained by a voltage divider. The input window and the drift electrode-1 are grounded. The drift electrode-2 is held at negative potential (≃ -1.5 kV) or at positive potential (+ 1.0 kV), depending on the fact whether the drift gap (drift electrode-1 - drift electrode-2) is switched on or off.

2.2. Delay line readout

The delay line readout from MWPCs has been succesfully used in many applications [4 ÷ 10]. Delay line readout is a good compromise between the requirements, such as the spatial resolution, the count rate capability and the cost. The spatial resolution of 0.1% of the total coordinate length and count rate up to 10^6 events/s are achievable with this method. A disadvantage of the delay line is that it needs the higher gas gain in comparison with the centre of gravity method[11,12] to get a high spatial resolution . In the case of the neutron detection the requirement to spatial resolution is not so strict. Taking into account the spatial resolution of primary ionization it is possible to operate the detector at a moderate signal/noise ratio. A specific delay τ = 1.0/mm has been chosen. It provides sufficient resolution < 1 mm. The attenuation of delay lines (connected with the MWPC) is ≃ 20%. The rise-time of cathode signals from the preamplifier is ≃35 ns; measured for neutrons with the gas mixture 3.0atm. He+ + 1.5 atm. propane.

2.3. Detector's electronic system

The electronic system is designed for the coordinate readout and data acquisition in the form of a two-dimensional image. The main advantage of the delay line readout method can be seen in the fact, that a low number of readout channels is needed: only five channels in 2-D detectors. It simplifies readout electronics and the determination of coordinates of a detected particle leads to the precise measurements of time intervals between arrivals of signals to both ends of each delay line. The count rate capability of the detector with readout electronics is defined mainly by the total time delay of the used delay lines. The readout electronics adds 50 ÷ 100 ns to the total dead time, additionally, due to the veto logic.

Readout electronics (in CAMAC) involves the following units:

-low-noise preamplifiers (placed on the detector) and amplifiers (in the CAMAC crate);

-constant fraction discriminators;

-time-to-digital convertors (TDC) (one for each coordinate), which digitize time intervals between signal arrivals independently on the signal coming first; moreover, the veto logic and 3 fold FIFO memory are included in each TDC for proper event selection and derandomization of Poisson statistics of particle flux;

-histogramming memory;

-CAMAC crate controller interfacing a PC/AT computer .

Moreover, the electronic system includes H. V. power supply modules, a quad counter and some other auxiliery CAMAC

modules. All the electronics system is in two CAMAC crates, the first one is placed at the detector on the experimental channel. Five NIM-level signal from discriminators are led via coaxial cables to the second crate which is placed at the PC/AT in the distance of some meters.

Thus, neutron field map is acquired on line. A quick check of correct data acquisition at the experiment is provided by means of the fourfold counter , which displays counts in the anode channel and one of the cathode channels together with counts of "digitalizion enable" and "strobe of histogramming memory" signals. Relations of these counts to the anode count are automatically displayed on the PC during data acquisition and may indicate an unproper H.V.setting, discriminator adjustament, etc. The main parameters of the used readout electronics system are presented in Tab.1.

2.4. Software for the neutron PSD

The programm, written for the neutron PSD allows to control acquisition of 2-D patterns and its transmission to the PC/AT. Further it makes preliminary processing and displaying of the acquired 2-D pattern. It allows to make arithmetical operations (addition, subtraction, multiplication, division) with two matrix of 2-D pattern and to display a neutron field map on the PC/AT colour monitor. The programm searches minimum/maximum in a 2-D Region-Of-Interest (ROI), calculates the average count/pixel in a ROI and its standard deviation, displays cross-sectional histograms of a ROI. Later on searches peaks in the histogram

Table 1

Specifications of the electronics system

-number of spatial resolution elements:	$256 \times 256 (\times 2^{16})$
-integral non-linearity	<0.05 %
-rate capability (at 20% counting losses)	>200 kHz
-accuracy of the coordinate determination	<1 ns (FWHM)
-differential nonuniformity	$\sigma \leq 0.4$ %
-minimal time channel width	1 ns
-maximum coded time interval	12 bits(or 2.0μs)

Table 2

Specification of two-dimensional neutron detector

1.	Detector principle	MWPC with delay line readout
2.	Sensitive area	260 x 140 mm^2
3.	Number of resolution elements	250 x 72
4.	Pixel size	1.07 x 1.99 mm^2
5.	Gas mixture	3 atm. ^3He + 1.5÷2.2 atm.propane
6.	Detection effficiency(at λ=6 Å)	>80 %
7.	Background:	
	-in the laboratory	0.2-0.5 anode pulse/s (integral)
	-at experimental reactor	2.0÷20 anode pulse/s (integral)
		0.5÷3 selected events/s
8.	Count rate capability	≥200kHz of selected events
9.	Uniformity of detection efficiency	≤ 2.5 % all sensitive area
		< 2.0 % for x-coordinate
10.	Integral nonlinearity	≤ 0.2 %
11.	Spatial resolution: x-coordinate	≤2.0 mm (FWHM)
	y-coordinate	≤2.6 mm (FWHM)
12.	Dynamic range (due to background)	$\simeq 10^4$

and calculates their statistics (FWHM, centre-of-gravitity, integral counts).

3. DETECTION OF SLOW NEUTRONS

The detector is filled with gas mixture based on the isotope ^3He and propane. Neutrons are detected via the reaction $^3He + n \rightarrow {}^3H + p + 764$ keV. Resulting protons and tritons leave points of the interaction in the opposite directions and isotropically in the space. Each particle produces a track of ionization. About 3×10^4 ion pairs are released at the full absorption of the proton and triton in the gas. Due to the higher energy of the proton (573 keV), and its lower stopping power, the centroid of released ionization is displaced against the point of interaction. The obtained spatial resolution for neutrons, thus, corresponds to spatial distribution of centroids of ionization projections to a corresponding coordinate for many registrated neutrons. In the detector with 15 atm of pure ^3He the spatial resolution limit is about 3.0 mm (FWHM) [13]. The use of propane admixture at pressure of 0.5 ÷ 2.5 atm. to reduce the range of protons [14], seems to be the optimal choice. The spatial resolution in the range of 1.3÷2.0 mm [15] can be achieved. At once propane acts as a proper quenching gas to helium, and moreover has the minimal conversion efficiency for gamma background [16].

3.1. Detection of gamma background

It is possible to supposse that only photons at the energy higher than ≈ 100 keV, are able to cause some

background. The calculated probability of photon interactions in the energy range 0.1 ÷ 5 MeV (using data [17]) for the gas filling 3 atm.He + 1.5 atm. C_3H_8 decreases while photon energy increasing. For the given size of this detector it changes from 0.9×10^{-3} at 100 keV to 0.4×10^{-3} at 1.0 MeV. In effect, due to the photoeffect and Compton scattering, each photon interaction with the gas filling is accompanied by release of an electron, which can be detected.

On other hand, using results of the well studied effect of X- and γ-ray inducing emmision of electron from solids [18 - 21], we can estimate the contribution of electrons impacted from the input window and walls of the pressure vessel to the background in the neutron detector. Summarizing:

- -the energy spectrum of these electrons has a broad distribution with a peak, placed at 50 ÷ 90 % of the energy of gamma (E_γ) and more than 90% of electrons spreads mostly in the interval energy 0.2÷1.0 E_γ for E_γ > 100 keV;
- -mostly the electron yield is incresing while incresing of proton number Z;
- -the electron yield has a significant minimum for 100÷300 keV photon energy, depending on target Z and is quickly increasing up to about tenfolds at E_γ= 3 MeV;
- -for aluminium for E_γ = 100 keV and 1.0 MeV the electron yield is 0.2×10^{-3} and 7.3×10^{-3} electrons/photon, respectively, for a normaly incident beam, and 0.9×10^{-3} and 28.3×10^{-3} electron/photon for an isotropically incident beam.

It is possible to conclude that electrons released from the detector vessel material make a considerable part of the gamma background. The calculation and measurements of this effect have been reported for plastic tubes, frequently used in high energy experiments [22], even in the worse case (for the neutron detection) of argon/methane filling. According to this, the contribution of electrons released from tube walls to the total background, is predominating at the photon energy above 200 keV.

When the higher gamma background discrimination in a neutron PSD is needed, it will be necessary to take electrons released from vessel walls into account.

4.TESTS OF THE NEUTRON PSD

At the beginning the detector has been investegated and adjusted in the laboratory by means of gamma- and neutron-emitting radioisotopes. All the principle parameters: the spatial resolution of the detector and all the device, gas gain characteristics, the laboratory backround level, etc. have been checked. Further, the electronics has been adjusted together with the detector from the point of view of the spatial resolution and uniformity of detection efficiency. Some tests have been performed on the nuclear pulse reactor IBR-2 at JINR. Main characteristics have been checked again after the installation of the neutron PSD at the IRT reactor.

4.1. Preliminary laboratory tests

The intrinsic spatial resolution of the detector has been determined by means of a time-to-apmlitude converter and multichannel analyser, using ^{55}Fe (5.9 keV) and ^{241}Am (59.6 keV) radioisotopes. The resolution of 0.4 mm (FWHM) (fig.5) and 1.0 mm (FWHM), respectively, has been measured for gas mixture Ar/CH_4 (80/20) at pressure of 5 atm.. Together with the above mentioned electronics and PC, the resolution of 1.5 mm (FWHM) of 59.6 keV has been measured, including quantization of 1.0mm / 1 channel of the coordinate along anode wires.

The uniformity of the detector response in each image pixel to the uniform illumination (it is a measure of differential non-linearity) depends on many factors, including constant gas gain across the whole sensitive area. The standard deviation of anode signal amplitudes of 1.7% has been achieved across the whole sensitive area, scanning the detector by means of the collimated ^{55}Fe source. After the adjustement of electronics the differential non-linearity 1.8% and 2.6% has been achived for the coordinate along and across anode wires, respectively. To get the uniform response in each channel for the coordinate across anode wires at the uniform illumination of the detector, it was necessary to choose the same number of channels and the number of anode wires per unit length.

4.2.Preliminary tests with neutrons

Among the worse properties of gaseous detector we can include the effect of deterioration of the energy resolution, generally, with the increasing gas gain. Quantitatively it depends on many factors: the volume density of the primary ionization, the used gas mixture, even on its composition [23]. This effect is obvious at the detection of neutrons by means of the gas mixture based on ^3He, where the higher stopping power of the proton and triton is amplified by the higher gas pressure.

Using the gas mixture 0.1 atm ^3He + 2.9 atm ^4He + 1.5 atm C_3H_8 and the Ra-Be neutron source the energy resolution of the pulse height distribution of anode signals has been measured for slow neutrons, illuminating the whole detector area. The energy resolution of the 764 keV peak, corresponding to a "full absorption "of the proton and triton of 15 % (FWHM), has been measured at the collected charge from anode of $5 \times 10^5 e^-$ (with τ = 1μs).

Fig.4 illustrates the deterioration of the pulse high distribution of anode signals with the increasing anode potential. The difference between the anode and cathode potential is a)3.0 kV, b) 3.4 kV and c)3.8 kV, that corresponds to the charge (collected on the anode with τ = 1 μs) a) $6x10^5$ e^- b) $3x10^6 e^-$ and c) $1x10^7 e^-$. It can be explained that due to the resulting protons and tritons, the amplification of more densed ionization becomes to be saturated. And the ionization due to the electrons, (from photoeffect and Compton of gamma background keeps amplified without any significant saturation. The deterioration of the

energy resolution makes the discrimination of neutrons worse against gamma background, which accompanies each neutron source. The gas mixture used at these measurements, has very low detection efficiency to neutron (of about 1%), thus, the gamma background is exagerrated. Also the effect of partial saturation of the gas amplification is visible in fig.5, which shows the dependence of amplitude of anode signals on the anode potential. An apparent deviation from the exponential dependence begins at the charge collected on the anode (with τ = 1μs) of $1x10^6 \div 2x10^6$ electrons.

For the reliability of experimental results it is important to maintain good stability of the main parameters against the anode potential. Fig.6.a) shows the efficiency curve for neutrons which has been measured after the installation of the detector on the experimental channel. A plateau of 500 Volts can be distinguished, where a slope is $\leq$ 0.6 % / 100 V.

The detector connected with data acquisition electronics and PC/AT has been tested at higher count rates at pulse reactor IBR-2 (Dubna).The frequency of neutron pulses is 5 Hz and in the place where the detector was situated while testing more than 95% of neutron arrivals happened in the total time interval 0.27 s per each second. At 10 % counting losses 40 000 events/s have been recorded in the histogramming memory. It corresponds to the count rate of 150 000 event/s at a steady state nuclear reactor. The counting limitation of the described PSD causes due to the total delay of the DLs.

4.3. Backround properties

Fig.6.b shows the same efficiency curve as in fig.6.a in a semilogarithmic scale together with background at the diffractiometrical facility DNM1. In the plateu region the background makes 7 ÷ 25 imp./s as an integral count of anode signals without additional shielding of the input window. The detection efficiency for neutrons was < 10 %, that deteriorates neutrons/background ratio. With the supplement shielding tube around the input window the average background outside of neutron spots varies from $3x10^{-5}$ to $2x10^{-4}$ counts/s/pixel. It corresponds to the background count 0.6 ÷ 4 counts/s, it is 10 times better, than anode count only. It results in the estimated neutron signal/backgroud ratio of about 10000 ÷ 1. Really, latter it was achieved with the fully ^3He filling.

The background at the experimental channel in the environment of the pulse reactor IBR-2 was changing from 2.0 to 15 anode pulse/s without additional timing discrimination and depended on the shielding and allocation of the detector. When the reactor was off, the background was about 0.2 ÷ 1.0 anode pulse/s.

4.4. Imaging properties of the neutron PSD

The detector has been filled with the gas mixture 3.0 atm. ^3He + 2.2 atm. C_3H_8. The spatial resolution of the detector working on line with a PC/AT is demonstrated in fig. 7.a,b. The neutron beam has been collimated by means of two parallel slits (0.3 mm wide) separated from each other in a

container with B_4C 10.0 mm placed before the detector window. By means of the time-to-amplitude converter and multichannel analyzer the spatial resolution of 1.4 mm (FWHM) has been measured for the "precise" coordinate along anode wires. When we take into account quantization of the system with PC/AT (1.0mm/channel and 2.0mm/channel) and the collimator width, this resolution corresponds to the measured value of 2.0 mm and 2.6 mm (FWHM) for the coordinate along and across anode wires (fig.7.a,b), respectively.

Fig.8 illustrates dependence of the spatial resolution for neutrons on the anode potential of the detector together with electronics. The cathode discriminators have been set to a threshold, which corresponds to the spatial resolution less than 1mm and by means of the anode discriminator has been set just above this value.

The integral nonlinearity of the detector has been measured in real geometry of SANS experiment. A cadmium sheet with precisely positioned holes of a 10.0 mm pitch has been fixed directly on the input window. The detector has been illuminated by neutrons scattered from a small parafin target placed in the neutron beam 20 x 20 mm^2 in size. The measured integral non-linearity (as maximum deviation from the linear fit related to the total length) does not exceed 0.2 %, including a paralax error caused by the thickness of the detector and the parafin target-detector distance of 1500 mm.

An example of SANR experiment is shown in fig.9 when a multilayer structure with periodicity of 60 Å on the glass substrate was investegated in two slit collimator geometry at λ = 2.2 Å. The higher peak corresponds to the direct neutron

beam passing through the substrate and the lower peak corresponds to the fraction reflected from the sample. At similar measurements the neutron PSD allows quickly to determine neutron intensity distribution of the primary, direct and reflected neutron beam. It is important for the evalution of the multilayer structure quality. The advantage of the neutron PSD can be seen in significant reduction of the time needed for the acquisition of sufficient statistics, especially, in wings of these distributions where few neutrons appear and the response is close to the background.

Fig.10 shows a 3-D view of the similar experiment. The Ioneda peak can be resolved in the valley between two higher peaks. This peak has not been observed at the comparative measurement while scanning of this part of space angle using the ^{3}He counter with a slit. It seems to happen due to unparallel geometry of the collimator, the counter slits and the sample, whose adjustment requires time for measuring. The two-dimensional PSD allows to simplify and speed-up these adjustments of the geometry.

5.CONCLUSIONS

This paper describes the two-dimensional slow neutron detector developed at JINR especially for SANS experiments. According to the first experience of its work in the experiment it is possible to conclude that delay line readout ensures sufficient parameters for relatively simple and reliable device for the purpose of SANS and SANR. This detector can be used for any conventional neutron diffraction

studies and for the acquisition of neutron tomography projection data of larger objects. Besides, this neutron PSD shows its advantage in measurements of low intensity neutron fields (above backround level) in the wide spatial angle at the condition of the DNM-1 facility. The main properties are summarized in Tab.II.

In these measurements where only one coordinate information would be sufficient for the estimation of the investigated effect, the 2-D detector has shown its advantage. 2-D data allow one to analyze the intensity distribution of scattered neutrons in slices perpendicular to the collimating slits. For example, we can evaluate some inhomogeneity across the sample area.

The detector with its software makes possible to fulfil quick and precize adjustment of the collimation system of the diffraction facility together with the sample, i.e. the localization of the sample to the maximum intensity of the beam is performed and the parallelism of the sample and slits is found.

6.ACKNOWLEDGEMENTS

The authors would like to thank Prof.A.M.Baldin for his continuous interest and support of our work and Dr.A.M.Balagurov, Dr. V.I.Gardelii, A.H.Ismailov, A.B.Kunchenko and Dr.V.G.Tishin for their assistance in tests at IBR-2 pulse reactor.

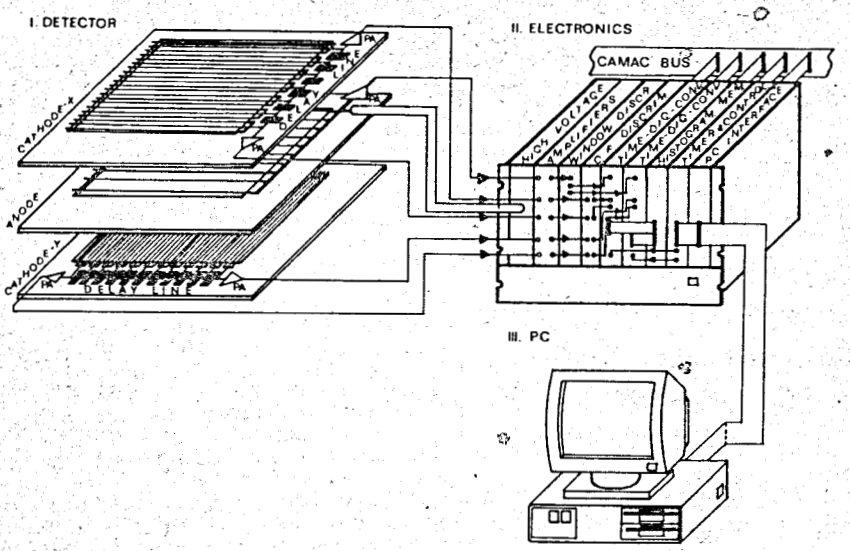

Fig.1. A schematic view of the two-dimensional detector with electronics and PC. In reality, the electronics is placed in two CAMAC crates. PA - preamplifier

Fig.2. A photograph of the detector without the front cover having the input window. Delay lines are visible with the connected cathode strips. Connections lead from each end of delay lines to feethrought connections can be seen for both coordinates. High voltage feethroughts are placed on the right side.

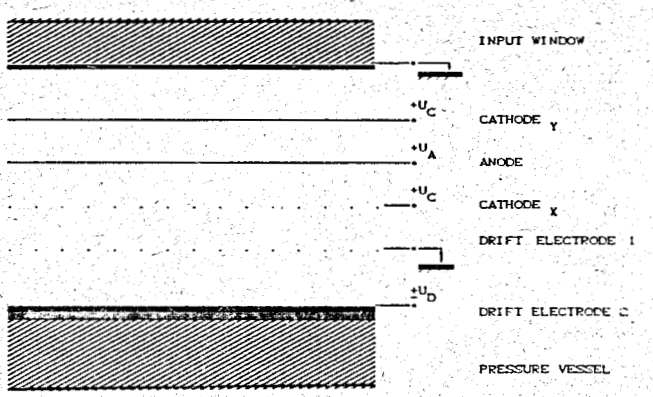

Fig.3. Schematic representation of the electrode geometry. Spacing between adjacent electrode is 4.0 mm, excluding drift electrode-1 ÷ drift electrode-2 gap which is 5 mm. Anode wire pitch is 2.0 mm, the pitch of other electrode 1.0 mm. Thickness of the aluminium input window 6 mm.

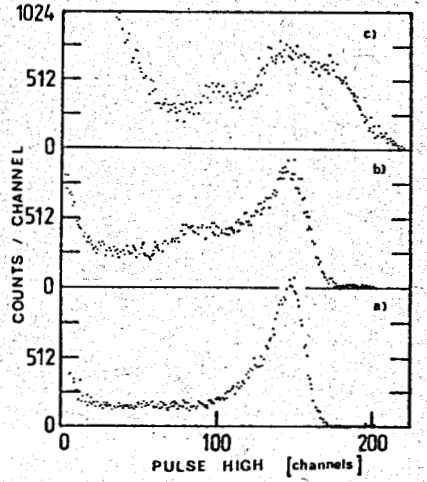

Fig.4. Pulse height spectra of anode signal at increasing anode potential. The gas mixture 0.1 atm ^{3}He and, 2.9 atm ^{4}He and 1.5 atm C_3H_8 has been used. The difference between anode and cathode potential is a) 3 kV, b) 3.4 kV and c) 3.8 kV.

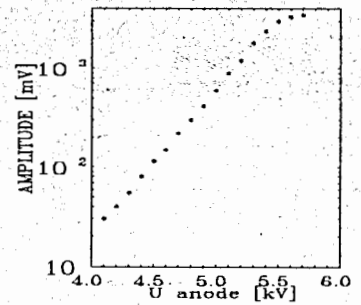

Fig.5. Pulse hight of anode signals vs. anode potential, measured with gas mixture 0.7 atm. ^{3}He +2.3atm. ^{4}He + 1.5atm.propane.

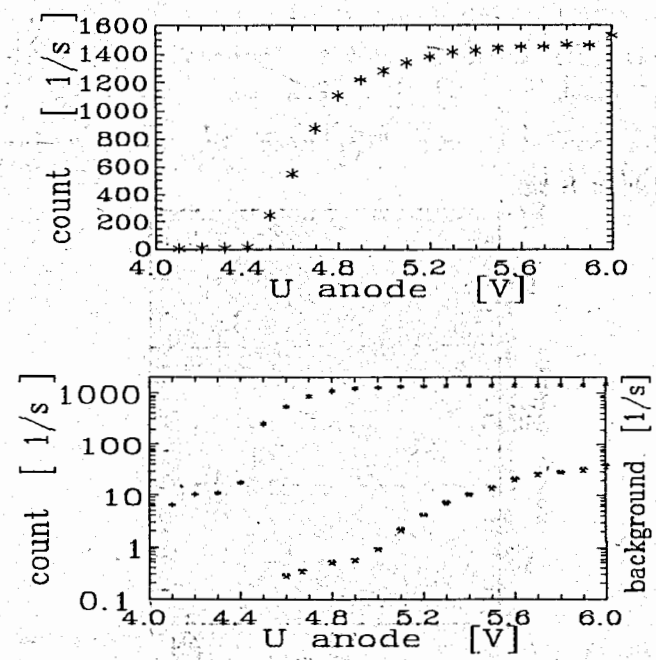

Fig.6. The efficiency curve for anode signals, measured in a broad neutron beam.a) in the linear scale;b) in logarithmic scale together with background

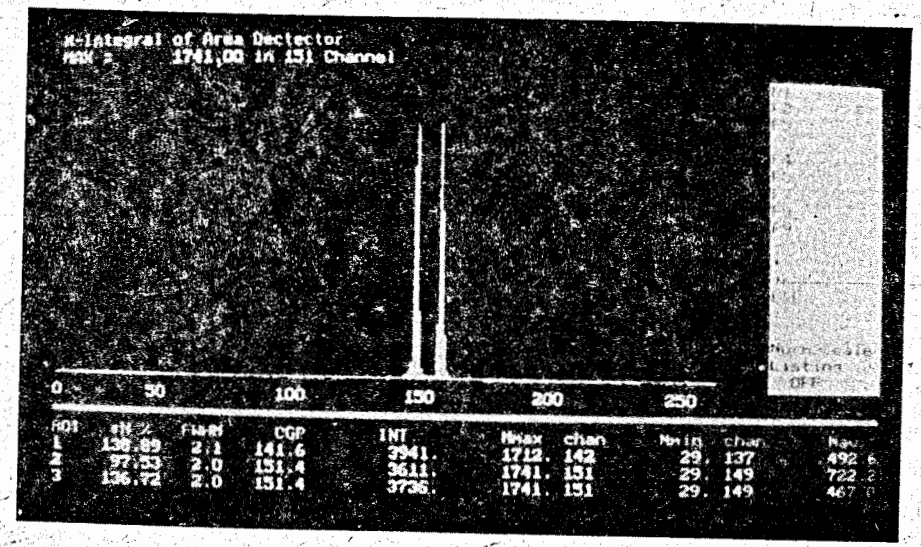

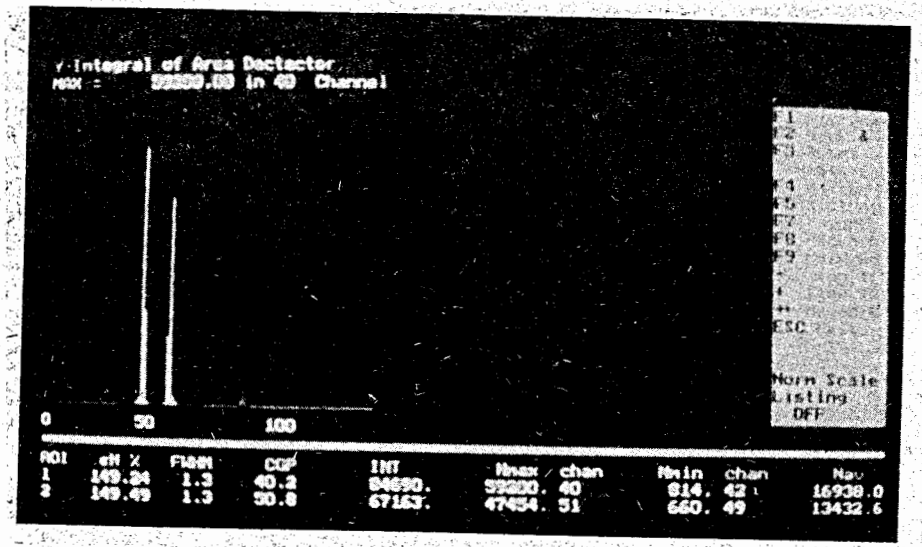

Fig.7. The neutron detector spatial response to a very narrow collimated neutron beam. Photographs are taken from a colour PC/AT monitor. a)for the "precise" x-coordinate (along anode wires);
b)for the y-coordinate across anode wires

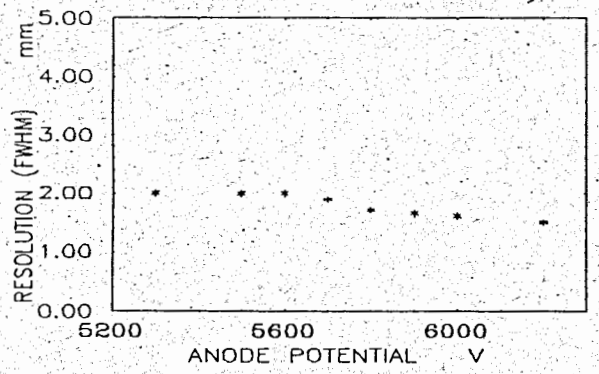

Fig.8. The dependence of the spatial resolution (including quantization of 1.0 mm/channel)on the anode potential.

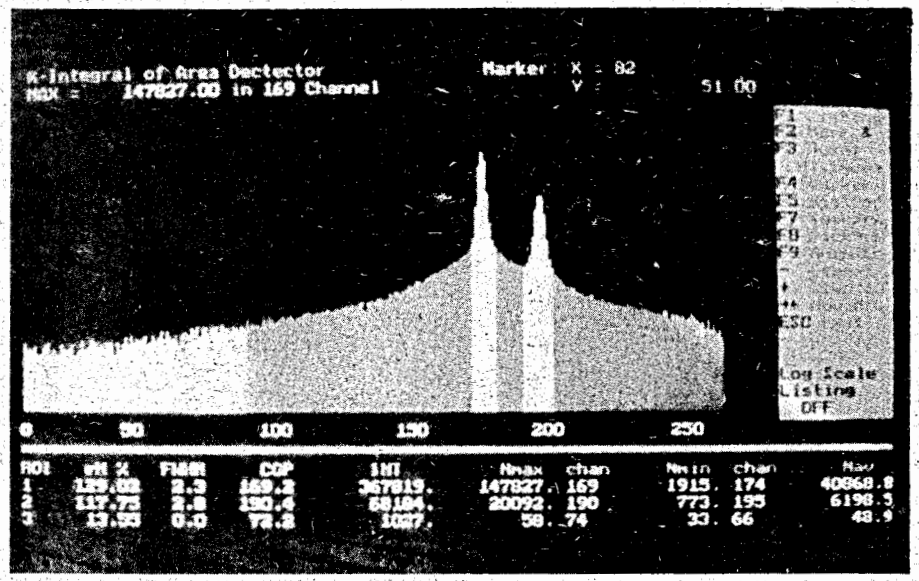

Fig.9. Example of the detector response at SANR experiment with a multilayer structure with periodicity of 60 Å. The photograph is taken from the PC monitor.

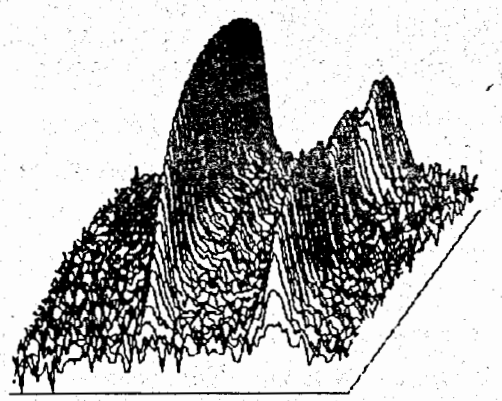

Fig.10. A 3-D view of the neutron field distribution of the direct and reflected beam from Cu-Ti structure.

REFERENCES

1. J.Plestil, Yu.M.Ostanevich, Yu.V.Bezzabotnov, D.Hlavata. Polymer 27(1986), 1241.
2. V.I. Gardeliy, V.G.Ivkov, Yu.M.Ostanevich and L.S.Jaguzhinskij. Biochimica et Biofisica Acta, vol.1061 (1991),p.39-48.
3. U.W.Arndt. Nucl.Instr.and Meth. A273 (1988), p. 459.
4. "Position-Sensitive Detection of Thermal Neutrons."edited by P.Convert and J.B.Forsyth. Academic Press. London 1983.
5. S.N.Kaplan, L.Kaufman, V.Perez-Mendez and K.Valentine. Nucl.Instr.and Meth. 106(1973), p. 397-406
6. Yu.V.Zanevsky, Chan Dyk Tkhan, G.A.Cheremukhina et al. Nucl.Instr.and Meth. A 283(1989), p. 463-466.
7. Yu.S.Anisimov, S.P.Chernenko, A.B.Ivanov, T.Netusil, et al. Nucl.Instr.and Meth. A 273(1988), p. 731-734.
8 V.Radeka. IEEE Trans.Nucl.Sci.NS-21 (1974), p.51-64.
9. J.E.Bateman, G.R.Moss, P.Rocket and S.Webb, Nucl. Inst. & Meth. A273 (1988), p.767-772.
10. R.Lewis, I.Sumner, A.Berry et al., Nucl.Inst. & Meth. A273(1988), p.773-777.

11. G.Charpak, G.Melchart, G.Peterson and F.Sauli. Nucl. Instr. & Meth. 167 (1979),p.455.
12. V.Radeka and R.A.Boie. Nucl.Instr.& Meth.,178 (1980), p.543.13. J.Jacobe, D.Feltin, A.Rambaud et al. in "Position-Sensitive Detection of Thermal Neutrons."edited by P.Convert and J.B.Forsyth. Academic Press. London 1983, p.106-119.
14. R.A.Boie, J.Fischer. Y.Inagaki, F.C.Merrit, H.Okuno, V.Radeka. Nucl. Instr. & Meth.. 200(1982), p. 533-545.
15. B.P.Schoeborn, J.Shefer, O.K.Schneider. Nucl.Inst. & Meth. A252, p.180-187.
16. J.Fischer, V.Radeka and R.A.Boie.in "Position-Sensitive Detection of Thermal Neutrons."edited by P.Convert and J.B.Forsyth. Academic Press. London 1983, p.129-140.
17. E.Storm and H.I.Israel."Photons Cross Sections, Nuclear Data Tables",Vol.A-7,No.6, Acadamic Press, New York (1970).
18. A.F.Akkerman, M.Ya.Grudskij and V.V.Smirnov. "Secondary Emission of Electrons from Solids Due to the Gamma-Radiation. (in Russian) Energoatomizdat, Moscow, 1986.
19. M.Nakamura. J.Appl.Phys. 54(1983),p.3141.
20. A.F.Akkerman, V.A.Botvin, M.Ya.Grudskii. Phys.Stat.Sol. 110(1982), p.285.
21. T.A.Dellin, Huddleson and Mac Callum. IEEE Trans.on Nucl.Sci., NS-22 (1975), p.2549.
22. M.Laakso, K.Kurvinen and R.Orava. Nucl. Instr. & Meth. A273(1988), p.325.
25. R.D.Ramsay and P.C.Agrawal. Nucl.Instr.&Meth. A 273(1988), p.326.

Received by Publishing Department
on February 11, 1992.